Correlating atom probe tomography with x-ray and electron spectroscopies to understand microstructure–activity relationships in electrocatalysts

Baptiste Gault,* Kevin Schweinar, Siyuan Zhang, Leopold Lahn, Christina Scheu, Se-Ho Kim, and Olga Kasian

The search for a new energy paradigm with net-zero carbon emissions requires new technologies for energy generation and storage that are at the crossroad between engineering, chemistry, physics, surface, and materials sciences. To keep pushing the inherent boundaries of device performance and lifetime, we need to step away from a cook-and-look approach and aim to establish the scientific ground to guide the design of new materials. This requires strong efforts in establishing bridges between microscopy and spectroscopy techniques, across multiple scales. Here, we discuss how the complementarities of x-ray- and electron-based spectroscopies and atom probe tomography can be exploited in the study of surfaces and subsurfaces to understand structure–property relationships in electrocatalysts.

Introduction

The technologies necessary for the electrification of transportation, the generation of green hydrogen at scale[1] for transport and manufacturing,[2] and the grid-scale energy storage to accommodate the intermittency of renewable electricity generation[3,4] all require new materials solutions.[5] The performance and service lifetime of these materials are inherently related to their microstructure, chemistry, physics, and interaction with their environment. Understanding the subtle processing–structure–property relationships is key to guide the design of future generations of materials. Yet, the variety of scales involved, from individual atoms to nano- to micro- to millimeter scales, and nature of the information—(i.e., surface atomic arrangements, crystalline structure, composition, and chemistry)—is simply too broad for a single technique to provide all the necessary insights. Hence, correlative approaches must be developed to build upon the strength of each individual technique, as showcased in the case of microstructural features found in the bulk of materials,[6] especially structural defects.[7–9] Another challenge is that a material's chemical (re) activity can be underpinned by metastable species at the surface of the electrodes and their analyses can only be performed by using *in situ* or *in operando* techniques.

Atom probe tomography (APT) provides three-dimensional compositional mapping of materials with subnanometer resolution[10] and as such is poised to provide extremely valuable insights. APT has progressively increased in prominence in the battery of characterization techniques for bulk metallic materials,[11–13] ceramics and semiconductors,[14,15] phase-change materials,[16] and with recent forays into nanostructures,[17,18] including nanoparticles[19–23] and 2D materials.[24,25] There are also numerous potential application in catalysis, as recently reviewed by Barroo et al.[26] There is a compatibility in scales between specimens for APT, shaped as sharp needles with a near-spherical cap at their end, and nanoparticles used

Baptiste Gault, Max-Planck-Institut für Eisenforschung, Düsseldorf, Germany; Department of Materials, Royal School of Mines, Imperial College London, London, UK; b.gault@mpie.de
Kevin Schweinar, Max-Planck-Institut für Eisenforschung, Düsseldorf, Germany; Stat Peel AG, Glarus, Switzerland; kevin.schweinar@statpeel.com
Siyuan Zhang, Max-Planck-Institut für Eisenforschung, Düsseldorf, Germany; siyuan.zhang@mpie.de
Leopold Lahn, Max-Planck-Institut für Eisenforschung, Düsseldorf, Germany; Helmholtz Institut Erlangen-Nürnberg, Helmholtz-Zentrum Berlin GmbH, Berlin, Germany; Department of Materials Science and Engineering, Friedrich-Alexander-Universität Erlangen-Nürnberg, Erlangen, Germany; leopold.lahn@helmholtz-berlin.de
Christina Scheu, Max-Planck-Institut für Eisenforschung, Düsseldorf, Germany; RWTH Aachen University, Aachen, Germany; scheu@mpie.de
Se-Ho Kim, Max-Planck-Institut für Eisenforschung, Düsseldorf, Germany; s.kim@mpie.de
Olga Kasian, Max-Planck-Institut für Eisenforschung, Düsseldorf, Germany; Helmholtz Institut Erlangen-Nürnberg, Helmholtz-Zentrum Berlin GmbH, Berlin, Germany; Department of Materials Science and Engineering, Friedrich-Alexander-Universität Erlangen-Nürnberg, Erlangen, Germany; olga.kasian@helmholtz-berlin.de
*Corresponding author

doi:10.1557/s43577-022-00373-8

© The Author(s) 2022

across many catalysis applications (i.e., 10–200 nm in diameter). Historically, this had enabled field-electron emission microscopy (FEEM/FEM) to be extensively used to study surfaces in reaction conditions.[27] The reacted surfaces were then imagined by field-ion microscopy (FIM) in search for morphological or atomic-scale topographical modifications. Early implementation of atom probes were then sometimes used to measure changes in the surface chemistry; however, they were limited to one-dimensional depth-profiling of the composition or to study a single set of reacted planes.[27]

The analysis of catalysts and electrocatalysts is, however, an area in which deploying the full potential of APT could be transformational. However, despite outstanding works performed in a limited number of groups,[28–31] APT has not seen a fast spread in surface sciences studies, in part because of difficulties in specimen preparation, but also a lack of direct structural information available along with the chemical and bonding state of surface species. These are accessible through x-ray photoelectron spectroscopy (XPS), one of the key techniques used in surface sciences. XPS allows access to the bonding state within the first few atomic layers of the surface. For its compatibility in scale, APT is more often correlated with (scanning) transmission electron microscopy, in which the bonding state can be obtained from electron energy-loss spectroscopy ((S)TEM–EELS).[32,33] Energy-dispersive x-ray spectroscopy is also accessible in the (S)TEM (STEM–EDS) to assess the local composition; we, however, herein focus on techniques enabling to access the bonding state. The complementarity between STEM–EDS and APT had previously been discussed.[34] Preliminary work on thin films[35,36] demonstrated the importance of combining XPS, STEM–EELS, and APT to get a holistic understanding of the microstructural origin or the materials performance and degradation mechanisms.

In this article, following a brief overview of the working principles of these techniques to help the reader get to speed, we discuss the complementarities of these techniques and showcase examples from the recent literature to provide a perspective on the strength of the correlative approaches.

Working principles and techniques' complementarity

Working principles

We briefly introduce the working principles of the techniques discussed next for nonexperts. This should in any case not be seen as an exhaustive overview of these techniques, merely a segue enabling to position the perspective on the correlative approaches. It should be stressed that these techniques cannot be deployed on the exact same specimen, in the same instrument, and simultaneously, but must be used successively.

APT

In APT, as schematically depicted in **Figure 1**a, the atoms leave the surface of a needle-shaped specimen successively in the form of ions under the influence of an intense electric field. Following field evaporation, these ions fly along well-defined trajectories[37,38] and are collected by a single-particle detector that records the impact position.[39] The field evaporation is time-controlled by using either fast voltage[40] or laser pulses[41,42] superimposed to a DC high-voltage, thereby enabling the identification of the elemental nature of each ion by time-of-flight mass spectrometry.[43] The results from an APT experiment take the form of a mass spectrum (i.e., a histogram of the number of ions detected at a certain mass-to-charge ratio), and a point cloud, built from the detector impact positions, providing the atomic distribution in three-dimensions,[44] as summarized in Figure 1b.

X-ray photoelectron and electron energy-loss spectroscopies

In XPS, a micron-to-millimeter-sized beam of x-rays is focused onto the sample's surface. Upon penetration, some electrons from the material itself absorb photons from the incoming beam and get ejected from the material (i.e., the photoelectric effect). By measuring the kinetic energy of the emitted electron, and knowing the energy of the incoming photon, the bonding energy can be readily determined.[46] This is schematically summarized in Figure 1c. XPS hence provides a precise account of the chemistry of the first few atomic layers at the specimen's surface, averaged over microns to millimeters of the surface depending on the setup that is used.[46] There are ongoing efforts to perform spatially resolved XPS experiments with a lateral resolution in the range of tens to hundreds of nanometers.[47] A clear strength of XPS is the possibility to be used *in operando* (i.e., at temperatures and gas pressures that can mimic service conditions) to provide a precise account of the evolution of the surface chemistry over the course of reactions.[48]

STEM–EELS can provide similar information: as the incoming electrons travel through the thin specimen, inelastic scattering causes the loss of amounts of energy that can be related to plasmons or to the ionization energy of specific species. Analyzing the spectrum of the kinetic energy of the electrons coming out of the specimen allows for determining the specimen's composition and bonding state of the different species present. As the electron beam in STEM is tightly focused and scanned across the specimen's surface, STEM–EELS enables mapping of the species potentially within each individual atomic column along the pathway of the electron beam,[49,50] as schematically shown in Figure 1d. There are also

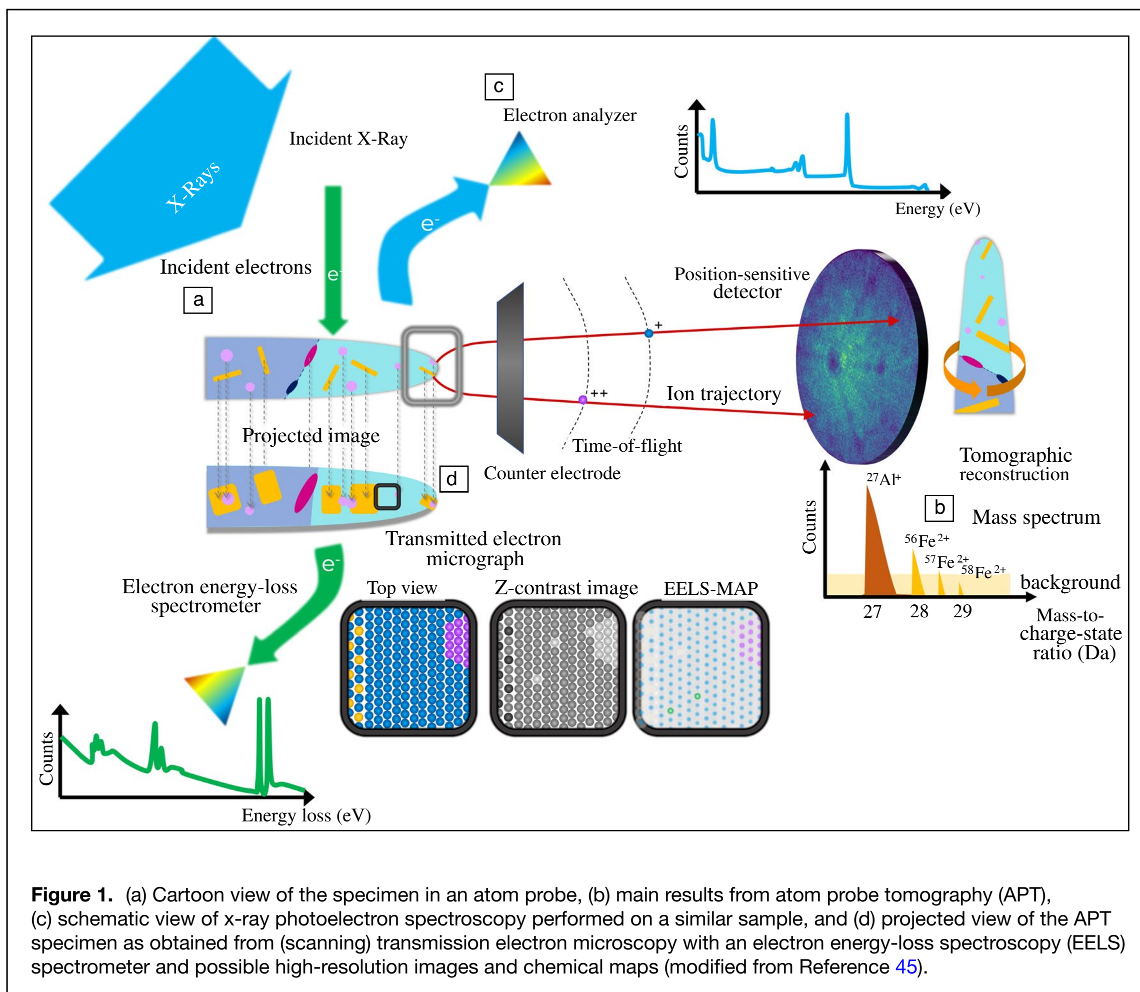

Figure 1. (a) Cartoon view of the specimen in an atom probe, (b) main results from atom probe tomography (APT), (c) schematic view of x-ray photoelectron spectroscopy performed on a similar sample, and (d) projected view of the APT specimen as obtained from (scanning) transmission electron microscopy with an electron energy-loss spectroscopy (EELS) spectrometer and possible high-resolution images and chemical maps (modified from Reference 45).

ongoing efforts to enable *in situ* or quasi *in operando* observations by STEM–EELS[51] to help better understand materials processes in conditions mimicking service.

Complementarities and challenges

First, there is a complementarity in the scale of the features that can be analyzed by the different techniques and a compatibility in the spatial resolutions. The spatial resolution of each of these techniques is anisotropic and depends on an array of parameters. What matters more is not the absolute value of the spatial resolution but the size of the smaller resolvable feature both laterally and in-depth. For both XPS and STEM–EELS, the spatial resolution not only depends on intrinsic instrumental parameters—the spot size of the illuminating beam, but also depends on extrinsic factors—for instance, the nature of the specimen itself. Indeed, in XPS, the penetration depth is dependent on the composition itself, typically below 10 nm, whereas the lateral extent depends on the size of the focused x-ray beam. In STEM–EELS, the signal collected is integrated through the thickness of the thin specimen (20–100 nm) and depends on the lateral extent of the focused electron beam, and its potential spread from scattering going through the specimen.[52] The actual spatial extent of the probed volume of the material can hence be difficult to ascertain. This is where the inherent strength of APT can be best used. In APT, the spatial resolution or size of the smaller resolvable microstructural feature of interest depends on its composition,[53,54] and it can be assumed to be below 1 nm in all three dimensions[55] but is typically an order of magnitude better in depth,[53,56] as summarized in **Figure 2**a.

Now, let us consider common microstructural features, for instance, stacking faults, dislocations, grain boundaries, and secondary phases, along with their respective dimensions, as shown in Figure 2b. The signal in the recorded spectra from XPS or STEM–EELS can be extremely complex as it is a combination of the signals originating from the features within the probed volume. Fitting approaches are hence used to decompose the signals originating from the different bulk or surface features averaged over the volume probed by the electron or x-ray beam.[33,50,57] This can lead to components and phases with a low volume fraction to be missed or overlooked, yet their influence on the materials properties may remain substantial.

This is where the correlation with APT can become a game changer: APT provides compositional mapping in three dimensions within the reconstructed volume, with a compositional sensitivity that can be in the range of parts-per-million,[58] and

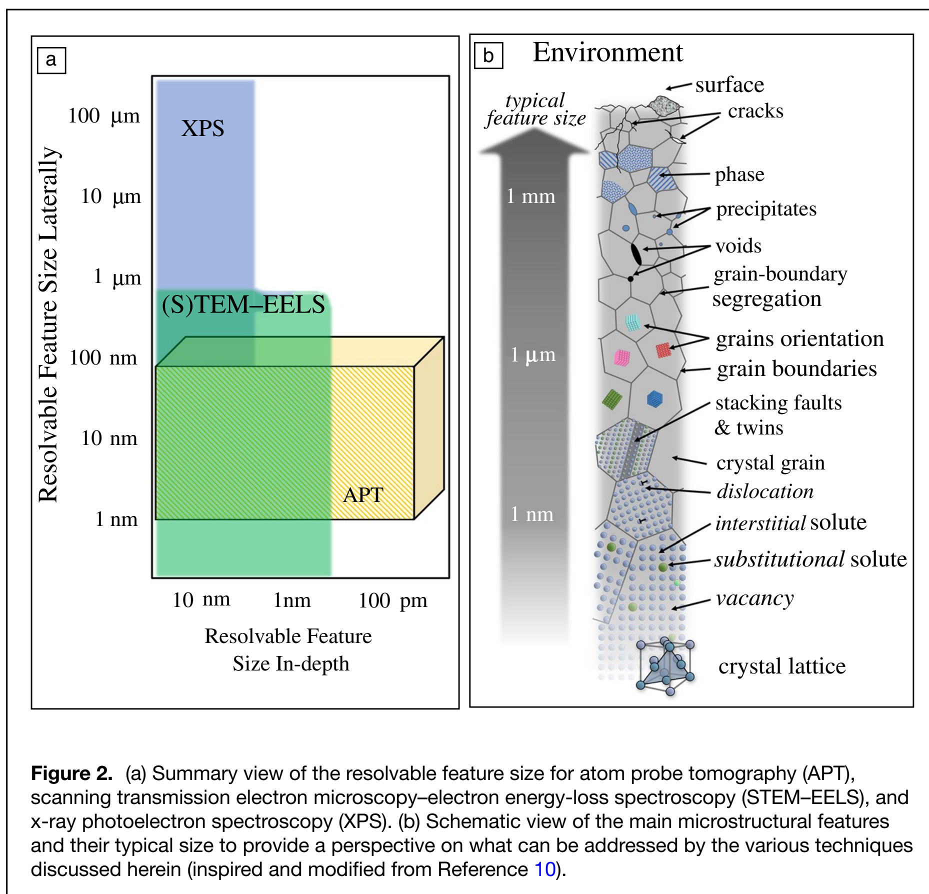

Figure 2. (a) Summary view of the resolvable feature size for atom probe tomography (APT), scanning transmission electron microscopy–electron energy-loss spectroscopy (STEM–EELS), and x-ray photoelectron spectroscopy (XPS). (b) Schematic view of the main microstructural features and their typical size to provide a perspective on what can be addressed by the various techniques discussed herein (inspired and modified from Reference 10).

individual features can be interrogated separately after data reconstruction and segmentation. This information can then be used to better understand the origins of the signal in the XPS or EELS spectrum. In turn, the bonding state remains inaccessible to APT. This is a first critical aspect of the complementarity with XPS and STEM–EELS, as the bonding state is required to understand the chemical activity or reactivity of a compound.

APT has a higher chemical sensitivity[58] than these spectroscopic techniques, especially for light elements (e.g., H,[59,60] C, and N).[61] Yet the compositional accuracy strongly depends on the local intensity of the electric field[62–64] during the analysis. These issues can make the analysis of certain materials or features challenging, and the complementary insights into the composition of some interfaces, for instance, that can be gleaned from STEM–EELS, can help support[65,66] the validity of some measurements.

Finally, the analysis of a sample's outermost surface requires dedicated strategies to avoid damage and contamination during specimen preparation and transport. For APT and STEM–EELS, specimens are typically prepared using a focused ion beam (FIB),[67,68] in which the energetic incoming ions get implanted, can cause amorphization, and can push surface atoms to penetrate inside the subsurface region.[69–71] The use of cryogenic temperatures during the preparation can help alleviate some issues,[72,73] but not all. A thin metallic coating can be used to protect the very surface, yet it often involves transporting the sample through ambient air, which can have an influence on the surface species themselves. There are efforts to develop approaches to transport samples under protective environments or (ultra-) high vacuum conditions and possibly under cryogenic conditions.[74–77] The use of transport suitcases has been more common in surface sciences, and most XPS instruments are equipped with an ion-gun to clean the specimen's surface by sputtering and remove the first few atomic layers.

Workflows and applications

Challenges arise in the development of appropriate workflows enabling analysis of the same sample to correlate the signals from the same microstructural features. Schweinar et al. proposed to use thin films deposited on the commercial flat-top coupons[78] used as support for APT specimen preparation,[79,80] as shown in **Figure 3**a. They performed spatially resolved XPS directly onto the film before and after thermal oxidation (Figure 3b–c), revealing the change in the oxidation state of Ir and Ru atoms. The compositional maps appear homogeneous across the 3-µm-wide disc at the top of the microtip. Following this analysis, the sample's surface was protected by a thin layer of sputter-deposited Cr and subsequently sharpened into an APT specimen by FIB[81] and analyzed by APT. The corresponding APT reconstruction is shown in Figure 3d. The analysis starts from the Cr capping layer, goes through the oxide layer, and terminates into the metallic film. Interestingly, by looking at a region of interest across the *x*–*y* section of the data set in the oxidized region, Ru is not spread across the material but rather agglomerated along grain boundaries within the thin film, as readily visible in Figure 3e. APT allows for quantification of the Ru segregation, determined as up to nearly 10 at.% (Figure 3f), accompanied by a depletion of Ir. This observation is likely related to the reduction in the free energy of the grain boundary associated with the segregation of Ru prior to oxidation.

This exemplifies the kind of insights that APT can bring—XPS could only detect a single oxide phase, whereas a richer microstructure is resolved by APT. The local changes in

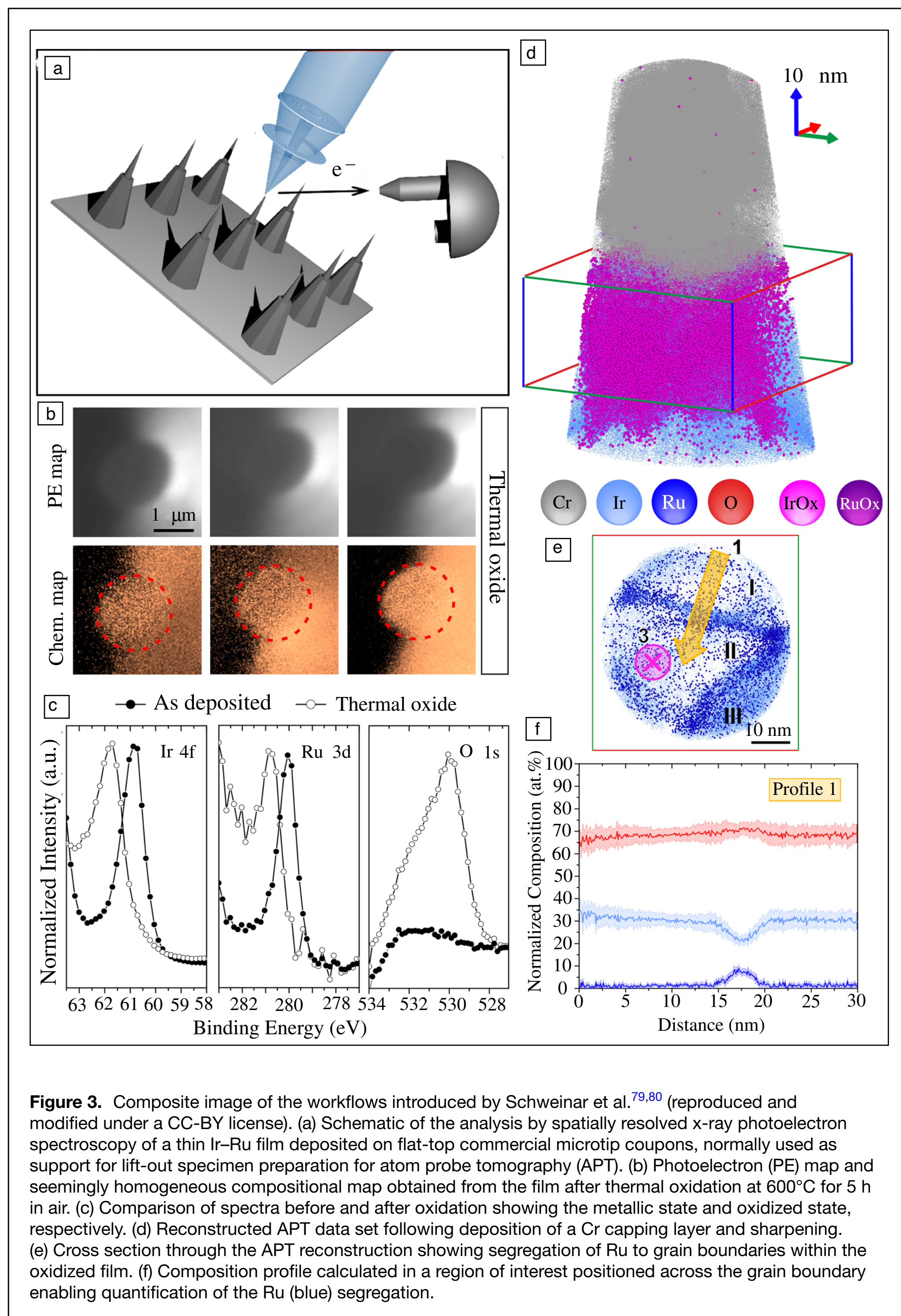

Figure 3. Composite image of the workflows introduced by Schweinar et al.[79,80] (reproduced and modified under a CC-BY license). (a) Schematic of the analysis by spatially resolved x-ray photoelectron spectroscopy of a thin Ir–Ru film deposited on flat-top commercial microtip coupons, normally used as support for lift-out specimen preparation for atom probe tomography (APT). (b) Photoelectron (PE) map and seemingly homogeneous compositional map obtained from the film after thermal oxidation at 600°C for 5 h in air. (c) Comparison of spectra before and after oxidation showing the metallic state and oxidized state, respectively. (d) Reconstructed APT data set following deposition of a Cr capping layer and sharpening. (e) Cross section through the APT reconstruction showing segregation of Ru to grain boundaries within the oxidized film. (f) Composition profile calculated in a region of interest positioned across the grain boundary enabling quantification of the Ru (blue) segregation.

composition at grain boundaries, combined with a different local atomic organization, will change the catalytic activity of the grain boundaries, as other studies have also shown with the aid of STEM–EELS.[35] If APT can be performed on a thin film suitable for XPS, the opposite was also proposed by Balakrishnan et al.,[82] in **Figure 4**a. They performed XPS first on APT specimens of Ir, which had been used as an electrocatalyst for the oxygen evolution reaction. Following XPS, the specimens were then analyzed by APT to reveal the local compositional evolution of the different sets of atomic planes that form the end surface of the needle.

Both of these approaches have advantages and drawbacks. For instance, the APT specimen's shape and size can make direct electrochemical or XPS measurements not necessarily straightforward, making the latter approach not always suitable, particularly when site-specific analysis is necessary. Yet the need to shape the specimen with a FIB after the reaction typically requires transporting the specimen through air, and the energetic ion beam can induce damage to the reacted sample's surface. Transport under protective atmospheres can be possible by using dedicated infrastructure[74] but it is not yet routinely available.

In any case, these studies showcased the spatial sensitivity of APT and the importance of the precise assessment of the species on the surface and in the near-surface regions. The depth probed by XPS is often not known precisely, as the penetration of the x-rays depends on the local composition and structure. In contrast, APT provides direct compositional measurement of the features on the surface, provided that appropriate protection is used prior to specimen preparation and analysis, and the spatial resolution of APT in the depth is extremely high.[54,56] There remains some uncertainties estimated to be 10% or more[84] in the

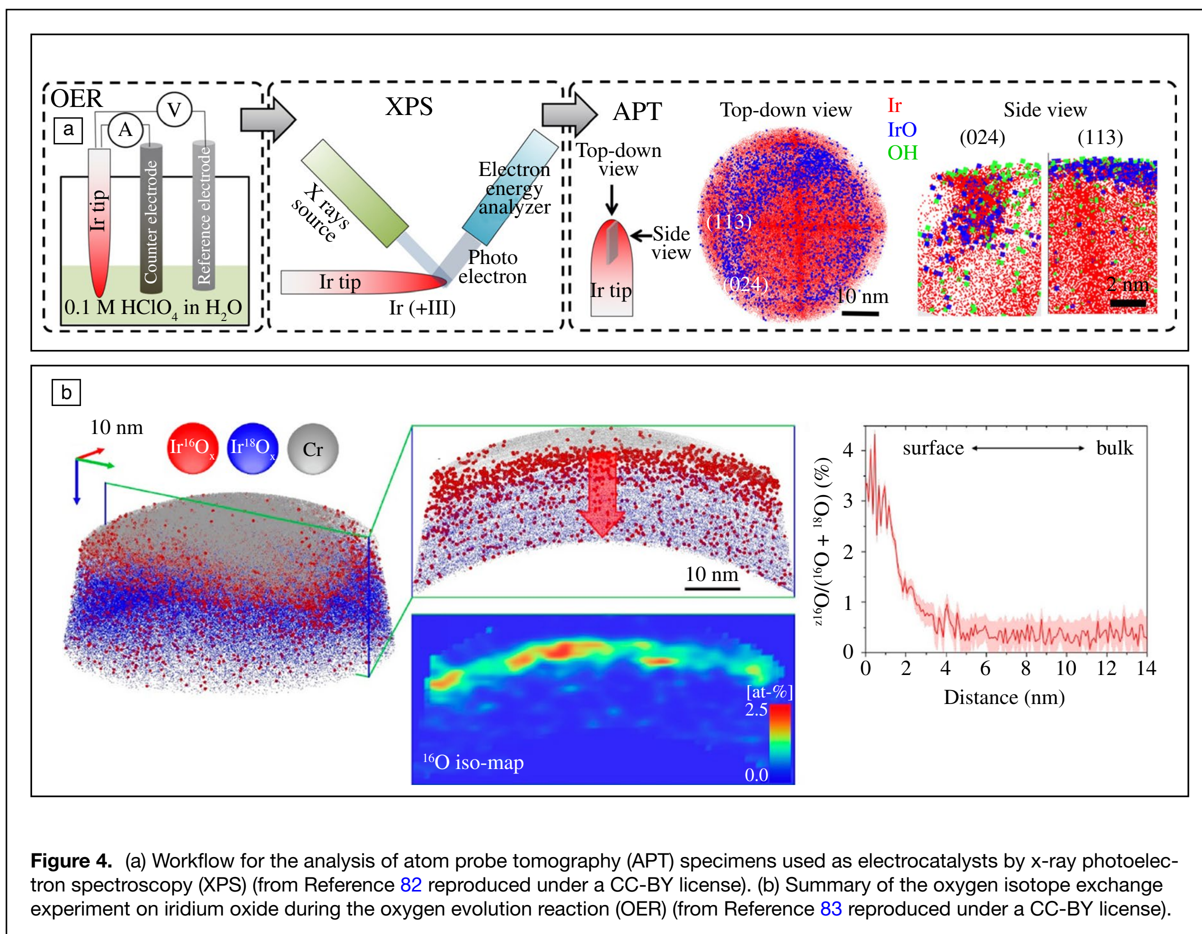

Figure 4. (a) Workflow for the analysis of atom probe tomography (APT) specimens used as electrocatalysts by x-ray photoelectron spectroscopy (XPS) (from Reference 82 reproduced under a CC-BY license). (b) Summary of the oxygen isotope exchange experiment on iridium oxide during the oxygen evolution reaction (OER) (from Reference 83 reproduced under a CC-BY license).

depth dimension of the APT reconstruction.[85] However, calibration of the spatial reconstruction parameters is possible either by using the partial structural information[86] from within the data or through the use of TEM.[6] This leads to an extreme spatial resolving power of APT that was, for instance, combined with isotope labeling to investigate the exchange of oxygen between the solution and the lattice of iridium oxide during the oxygen evolution reaction,[83] as summarized in Figure 4b.

Most showcase studies so far have focused on the analyses of electrocatalysts and electro-photo-catalysts that find application in the hydrogen energy cycle, especially the analysis of Ir metal in the form of thin films,[35] metal wire,[82] and mixed Ir–Ru alloys,[79] but also an array of oxides,[17,36,87–89] in particular to better understand the microstructural origins of their activity[36] or degradation in service.[88] In principle, similar approaches could be deployed in the future to a broad range of electro(photo)catalysts.

Conclusions

APT arises from FIM, and both were originally surface science techniques, yet progress in APT made the community progressively turn its attention toward bulk analyses. However, APT with its intrinsic capacity to map the composition or a material with a resolution better than a nanometer in three dimensions has great potential for complementing XPS that can probe the chemistry of a surface, and STEM–EELS, which provides compositional and chemical mapping through the thickness of a thin sample. Information from APT can guide the fitting of the electron energy spectra and facilitate data interpretation, as well as support investigation into processing–microstructure–property relationships that are necessary to design new electrocatalysts and electro-photo-catalysts. The difference in scale can be difficult to reconcile but the development of dedicated workflows has already enabled progress that will continue in the decade to come.

Acknowledgments

We thank U. Tezins, C. Broß, and A. Sturm for their support to the FIB and APT facilities at MPIE. We are grateful for the financial support from the BMBF via the project UGSLIT and the Max-Planck Gesellschaft via the Laplace project. S.-H.K. and B.G. acknowledge financial support from the ERC-CoG-SHINE-771602. K.S. is grateful for funding from the IMPRS-SurMat. BG is grateful to Jazmin Duarte for the initial version of Figure 2b.

Funding
Open Access funding enabled and organized by Projekt DEAL.

Conflict of interest
On behalf of all authors, the corresponding author states that there is no conflict of interest.

Open Access
This article is licensed under a Creative Commons Attribution 4.0 International License, which permits use, sharing, adaptation, distribution and reproduction in any medium or format, as long as you give appropriate credit to the original author(s) and the source, provide a link to the Creative Commons license, and indicate if changes were made. The images or other third party material in this article are included in the article's Creative Commons license, unless indicated otherwise in a credit line to the material. If material is not included in the article's Creative Commons license and your intended use is not permitted by statutory regulation or exceeds the permitted use, you will need to obtain permission directly from the copyright holder. To view a copy of this license, visit http://creativecommons.org/licenses/by/4.0/.

References
1. N. Danilovic, K.E. Ayers, C. Capuano, J.N. Renner, L. Wiles, M. Pertoso, *ECS Trans.* **75**, 395 (2016). https://doi.org/10.1149/07514.0395ecst
2. V. Vogl, M. Åhman, L.J. Nilsson, *J. Clean. Prod.* **203**, 736 (2018). https://doi.org/10.1016/j.jclepro.2018.08.279
3. M. Armand, J.M. Tarascon, *Nature* **414**, 359 (2001). https://doi.org/10.1038/35104644
4. J.M. Tarascon, M. Armand, *Nature* **451**, 652 (2008). https://doi.org/10.1038/451652a
5. D. Larcher, J.-M. Tarascon, *Nat. Chem.* **71**(7), 19 (2014). https://doi.org/10.1038/nchem.2085
6. M. Herbig, *Scr. Mater.* **148**, 98 (2018). https://doi.org/10.1016/J.SCRIPTAMAT.2017.03.017
7. M. Kuzmina, M. Herbig, D. Ponge, S. Sandlobes, D. Raabe, *Science* **349**, 1080 (2015). https://doi.org/10.1126/science.aab2633
8. S.K. Makineni, A. Kumar, M. Lenz, P. Kontis, T. Meiners, C. Zenk, S. Zaefferer, G. Eggeler, S. Neumeier, E. Spiecker, D. Raabe, B. Gault, *Acta Mater.* **155**, 362 (2018). https://doi.org/10.1016/J.ACTAMAT.2018.05.074
9. X. Zhou, J.R. Mianroodi, A. Kwiatkowski da Silva, T. Koenig, G.B. Thompson, P. Shanthraj, D. Ponge, B. Gault, B. Svendsen, D. Raabe, *Sci. Adv.* **7**, eabf0563 (2021). https://doi.org/10.1126/sciadv.abf0563
10. B. Gault, A. Chiaramonti, O. Cojocaru-Mirédin, P. Stender, R. Dubosq, C. Freysoldt, S.K. Makineni, T. Li, M. Moody, J.M. Cairney, *Nat. Rev. Methods Primers* **1**, 51 (2021)
11. D.N. Seidman, *Annu. Rev. Mater. Res.* **37**, 127 (2007). https://doi.org/10.1146/annurev.matsci.37.052506.084200
12. E.A. Marquis, M.K. Miller, D. Blavette, S.P. Ringer, C.K. Sudbrack, G.D.W. Smith, *MRS Bull.* **34**(10), 725 (2009)
13. P. Kürnsteiner, M.B. Wilms, A. Weisheit, B. Gault, E.A. Jägle, D. Raabe, *Nature* **582**, 515 (2020). https://doi.org/10.1038/s41586-020-2409-3
14. L.J. Lauhon, P. Adusumilli, P. Ronsheim, P.L. Flaitz, D. Lawrence, *MRS Bull.* **34**(10), 738 (2009)
15. D.J. Larson, A. Cerezo, J. Juraszek, K. Hono, G. Schmitz, *MRS Bull.* **34**(10), 732 (2009)
16. O. Cojocaru-Mirédin, H. Hollermann, A.M. Mio, A.Y.T. Wang, M. Wuttig, *J. Phys. Condens. Matter* **31**, 204002 (2019). https://doi.org/10.1088/1361-648X/AB078B
17. J. Lim, S.-H. Kim, R. Aymerich Armengol, O. Kasian, P.-P. Choi, L.T. Stephenson, B. Gault, C. Scheu, *Angew. Chem. Int. Ed.* (2020). https://doi.org/10.1002/anie.201915709
18. S.-H. Kim, S.-H. Yoo, P. Chakraborty, J. Jeong, J. Lim, A.A. El-Zoka, L.T. Stephenson, T. Hickel, J. Neugebauer, C. Scheu, M. Todorova, B. Gault, *J. Am. Chem. Soc.* **144**, 987 (2022). https://doi.org/10.1021/jacs.1c11680
19. K. Tedsree, T. Li, S. Jones, C.W.A. Chan, K.M.K. Yu, P.A.J. Bagot, E.A. Marquis, G.D.W. Smith, S.C.E. Tsang, *Nat. Nanotechnol.* **6**, 302 (2011). https://doi.org/10.1038/nnano.2011.42
20. S.-H.H. Kim, P.W. Kang, O.O. Park, J.-B.B. Seol, J.-P.P. Ahn, J.Y. Lee, P.-P.P. Choi, *Ultramicroscopy* **190**, 30 (2018). https://doi.org/10.1016/J.ULTRAMIC.2018.04.005
21. K. Jang, S.-H. Kim, H. Jun, C. Jung, J. Yu, S. Lee, P.-P. Choi, *Nat. Commun.* **12**, 5521 (2021)
22. T. Li, P.A.J. Bagot, E. Christian, B.R.C. Theobald, J.D.B. Sharman, D. Ozkaya, M.P. Moody, S.C.E. Tsang, G.D.W. Smith, *ACS Catal.* **4**, 695 (2014). https://doi.org/10.1021/cs401117e
23. P. Felfer, P. Benndorf, A. Masters, T. Maschmeyer, J.M. Cairney, *Angew. Chem. Int. Ed. Engl.* **53**, 11190 (2014). https://doi.org/10.1002/anie.201405043
24. M. Raghuwanshi, O. Cojocaru-Mirédin, M. Wuttig, *Nano Lett.* **20**, 116 (2020). https://doi.org/10.1021/acs.nanolett.9b03435
25. S.-H. Kim, J. Lim, R. Sahu, O. Kasian, L.T. Stephenson, C. Scheu, B. Gault, *Adv. Mater.* **32**(8), 1907235 (2020). https://doi.org/10.1002/adma.201907235
26. C. Barroo, A.J. Akey, D.C. Bell, *Appl. Sci.* **9**(13), 2721 (2019). https://doi.org/10.3390/app9132721
27. N. Kruse, *Ultramicroscopy* **89**, 51 (2001). https://doi.org/10.1016/S0304-3991(01)00119-X
28. P.A.J. Bagot, A. Cerezo, G.D.W. Smith, *Surf. Sci.* **601**, 2245 (2007). https://doi.org/10.1016/j.susc.2007.03.030
29. M. Moors, T.V. de Bocarmé, N. Kruse, *Catal. Today* **124**, 61 (2007). https://doi.org/10.1016/j.cattod.2007.01.063
30. T. Li, E.A. Marquis, P.A.J. Bagot, S.C. Tsang, G.D.W. Smith, *Catal. Today* **175**, 552 (2011). https://doi.org/10.1016/j.cattod.2011.03.046
31. P.A.J. Bagot, A. Cerezo, G.D.W. Smith, T.V. de Bocarmé, T.J. Godfrey, *Surf. Interface Anal.* **39**, 172 (2007). https://doi.org/10.1002/sia.2484
32. M. Kociak, O. Stéphan, *Chem. Soc. Rev.* **43**, 3865 (2014). https://doi.org/10.1039/c3cs60478k
33. S. Zhang, C. Scheu, *Microscopy* **67**, i133 (2018). https://doi.org/10.1093/jmicro/dfx091
34. W. Guo, B.T. Sneed, L. Zhou, W. Tang, M.J. Kramer, D.A. Cullen, J.D. Poplawsky, *Microsc. Microanal.* **22**, 1251 (2016). https://doi.org/10.1017/S1431927616012496
35. T. Li, O. Kasian, S. Cherevko, S. Zhang, S. Geiger, C. Scheu, P. Felfer, D. Raabe, B. Gault, K.J.J. Mayrhofer, *Nat. Catal.* **1**, 300 (2018). https://doi.org/10.1038/s41929-018-0043-3
36. B. Scherrer, T. Li, A. Tsyganok, M. Döbeli, B. Gupta, K.D. Malviya, O. Kasian, N. Maman, B. Gault, D.A. Grave, D. Raabe, A. Rothschild, A. Mehlman, I. Visoly-Fisher, D. Raabe, A. Rothschild, *Chem. Mater.* **32**, 1031 (2020). https://doi.org/10.1021/acs.chemmater.9b03704
37. F. Vurpillot, A. Bostel, D. Blavette, *Appl. Phys. Lett.* **76**, 3127 (2000)
38. C. Fletcher, M.P. Moody, D. Haley, *J. Phys. D* **52**, 435305 (2019). https://doi.org/10.1088/1361-6463/ab3703
39. G. Da Costa, F. Vurpillot, A. Bostel, M. Bouet, B. Deconihout, *Rev. Sci. Instrum.* **76**, 13304 (2005). https://doi.org/10.1063/1.1829975
40. B. Ravelo, F. Vurpillot, *Prog. Electromagn. Res. Lett.* **47**, 61 (2014). https://doi.org/10.2528/PIERL14042403
41. B. Gault, F. Vurpillot, A. Vella, M. Gilbert, A. Menand, D. Blavette, B. Deconihout, *Rev. Sci. Instrum.* **77**, 43705 (2006). https://doi.org/10.1063/1.2194089
42. J.H. Bunton, J.D. Olson, D.R. Lenz, T.F. Kelly, *Microsc. Microanal.* **13**, 418 (2007). https://doi.org/10.1017/S1431927607070869
43. E.W. Müller, J.A. Panitz, S.B. McLane, E.W. Müller, *Rev. Sci. Instrum.* **39**, 83 (1968). https://doi.org/10.1063/1.1683116
44. B. Gault, D. Haley, F. De Geuser, M.P. Moody, E.A. Marquis, D.J. Larson, B.P. Geiser, *Ultramicroscopy* **111**, 448 (2011). https://doi.org/10.1016/j.ultramic.2010.11.016
45. D. Raabe, D. Ponge, P.J. Uggowitzer, M. Roscher, M. Paolantonio, C. Liu, H. Antrekowitsch, E. Kozeschnik, D. Seidmann, B. Gault, F. De Geuser, A. Deschamps, C. Hutchinson, C. Liu, Z. Li, P. Prangnell, J. Robson, P. Shanthraj, S. Vakili, C. Sinclair, L. Bourgeois, S. Pogatscher, *Prog. Mater. Sci.* **128**, 100947 (2022). https://doi.org/10.1016/J.PMATSCI.2022.100947
46. G. Greczynski, L. Hultman, *Prog. Mater. Sci.* **107**, 100591 (2020). https://doi.org/10.1016/J.PMATSCI.2019.100591
47. M. Amati, B. Aleman, B. Bozzini, L. Gregoratti, H. Sezen, M. Kiskinova, *Surf. Sci.* **652**, 20 (2016). https://doi.org/10.1016/J.SUSC.2016.01.017
48. C. Papp, H.P. Steinrück, *Surf. Sci. Rep.* **68**, 446 (2013). https://doi.org/10.1016/J.SURFREP.2013.10.003
49. S.J. Pennycook, M. Varela, C.J.D. Hetherington, A.I. Kirkland, *MRS Bull.* **31**(1), 36 (2006). https://doi.org/10.1557/mrs2006.4
50. M. Kociak, O. Stéphan, M.G. Walls, M. Tencé, C. Colliex, in *Scanning Transmission Electron Microscopy* (Springer, New York, 2011), pp. 163–205. https://doi.org/10.1007/978-1-4419-7200-2_4
51. M.E. Holtz, Y. Yu, J. Gao, H.D. Abruña, D.A. Muller, *Microsc. Microanal.* **19**, 1027 (2013). https://doi.org/10.1017/S1431927613001505
52. D.T. Nguyen, S.D. Findlay, J. Etheridge, *Ultramicroscopy* **184**, 143 (2018). https://doi.org/10.1016/j.ultramic.2017.08.020

53. B. Gault, B. Klaes, F.F. Morgado, C. Freysoldt, Y. Li, F. De Geuser, L.T. Stephenson, F. Vurpillot, *Microsc. Microanal.* **28**(4), 1116 (2022). https://doi.org/10.1017/S1431927621012952
54. B.M. Jenkins, F. Danoix, M. Gouné, P.A.J. Bagot, Z. Peng, M.P. Moody, B. Gault, *Microsc. Microanal.* **26**, 247 (2020). https://doi.org/10.1017/s1431927620000197
55. F. De Geuser, B. Gault, *Acta Mater.* **188**, 406 (2020). https://doi.org/10.1016/j.actamat.2020.02.023
56. B. Gault, M.P. Moody, F. De Geuser, A. La Fontaine, L.T. Stephenson, D. Haley, S.P. Ringer, *Microsc. Microanal.* **16**, 99 (2010). https://doi.org/10.1017/S1431927609991267
57. G.H. Major, N. Fairley, P.M.A. Sherwood, M.R. Linford, J. Terry, V. Fernandez, K. Artyushkova, *J. Vac. Sci. Technol. A* **38**, 061203 (2020). https://doi.org/10.1116/6.0000377
58. D. Haley, A.J. London, M.P. Moody, *Microsc. Microanal.* **26**(5), 964 (2020). https://doi.org/10.1017/S1431927620024290
59. Y.S. Chen, P.A.J. Bagot, M.P. Moody, D. Haley, *Int. J. Hydrogen Energy* **44**, 32280 (2019). https://doi.org/10.1016/j.ijhydene.2019.09.232
60. A.J. Breen, L.T. Stephenson, B. Sun, Y. Li, O. Kasian, D. Raabe, M. Herbig, B. Gault, *Acta Mater.* **188**, 108 (2020). https://doi.org/10.1016/j.actamat.2020.02.004
61. W. Sha, L. Chang, G.D.W. Smith, C. Liu, E.J.J. Mittemeijer, *Surf. Sci.* **266**, 416 (1992). https://doi.org/10.1016/0039-6028(92)91055-G
62. B. Gault, D.W. Saxey, M.W. Ashton, S.B. Sinnott, A.N. Chiaramonti, M.P. Moody, D.K. Schreiber, *New J. Phys.* **18**, 033031 (2016). https://doi.org/10.1088/1367-2630/18/3/033031
63. D. Zanuttini, I. Blum, L. Rigutti, F. Vurpillot, J. Douady, E. Jacquet, P.-M. Anglade, B. Gervais, *Phys. Rev. A* **95**, 61401 (2017). https://doi.org/10.1103/PhysRevA.95.061401
64. Z. Peng, D. Zanuttini, B. Gervais, E. Jacquet, I. Blum, P.P. Choi, D. Raabe, F. Vurpillot, B. Gault, *J. Phys. Chem. Lett.* **10**, 581 (2019). https://doi.org/10.1021/acs.jpclett.8b03449
65. F. Danoix, X. Sauvage, D. Huin, L. Germain, M. Gouné, *Scr. Mater.* **121**, 61 (2016). https://doi.org/10.1016/J.SCRIPTAMAT.2016.04.038
66. A.J. Craven, M. MacKenzie, A. Cerezo, T. Godfrey, P.H. Clifton, *Mater. Sci. Technol.* **24**, 641 (2008). https://doi.org/10.1179/174328408X270347
67. C.R. Hutchinson, R.E. Hackenberg, G.J. Shiflet, *Ultramicroscopy* **94**, 37 (2003). https://doi.org/10.1016/S0304-3991(02)00193-6
68. K. Thompson, D. Lawrence, D.J. Larson, J.D. Olson, T.F. Kelly, B. Gorman, *Ultramicroscopy* **107**, 131 (2007). https://doi.org/10.1016/j.ultramic.2006.06.008
69. Y. Chang, W. Lu, J. Guénolé, L.T. Stephenson, A. Szczpaniak, P. Kontis, A.K. Ackerman, F. Dear, I. Mouton, X. Zhong, D. Raabe, B. Gault, S. Zhang, D. Dye, C.H. Liebscher, D. Ponge, S. Korte-Kerze, D. Raabe, B. Gault, *Nat. Commun.* **10**, 942 (2019). https://doi.org/10.1038/s41467-019-08752-7
70. O. Cojocaru-Mirédin, T. Schwarz, D. Abou-Ras, *Scr. Mater.* **148**, 106 (2018). https://doi.org/10.1016/j.scriptamat.2017.03.034
71. D.J. Larson, D.T. Foord, A.K. Petford-Long, H. Liew, M.G. Blamire, A. Cerezo, G.D.W. Smith, *Ultramicroscopy* **79**, 287 (1999). https://doi.org/10.1016/S0304-3991(99)00055-8
72. N.A. Rivas, A. Babayigit, B. Conings, T. Schwarz, A. Sturm, A.G. Manjón, O. Cojocaru-Mirédin, B. Gault, F.U. Renner, *PLoS One* **15**, e0227920 (2020). https://doi.org/10.1371/journal.pone.0227920
73. L. Lilensten, B. Gault, *PLoS One* **15**(4), e0231179 (2020). https://doi.org/10.1371/journal.pone.0231179
74. L.T. Stephenson, A. Szczepaniak, I. Mouton, K.A.K. Rusitzka, A.J. Breen, U. Tezins, A. Sturm, D. Vogel, Y. Chang, P. Kontis, A. Rosenthal, J.D. Shepard, U. Maier, T.F. Kelly, D. Raabe, B. Gault, *PLoS One* **13**, e0209211 (2018). https://doi.org/10.1371/journal.pone.0209211
75. A.A. El-Zoka, S.-H. Kim, S. Deville, R.C. Newman, L.T. Stephenson, B. Gault, *Sci. Adv.* **6**(49), eabd6324 (2020). https://doi.org/10.1126/sciadv.abd6324
76. I.E. McCarroll, P.A.J. Bagot, A. Devaraj, D.E. Perea, J.M. Cairney, *Mater. Today Adv.* **7**, 100090 (2020). https://doi.org/10.1016/j.mtadv.2020.100090
77. D.E. Perea, S.S.A. Gerstl, J. Chin, B. Hirschi, J.E. Evans, *Adv. Struct. Chem. Imaging* **3**, 12 (2017). https://doi.org/10.1186/s40679-017-0045-2
78. K. Thompson, D.J. Larson, R.M. Ulfig, *Microsc. Microanal.* **11**, 882 (2005). https://doi.org/10.1017/S1431927605502629
79. K. Schweinar, R.L. Nicholls, C.R. Rajamathi, P. Zeller, M. Amati, L. Gregoratti, D. Raabe, M. Greiner, B. Gault, O. Kasian, *J. Mater. Chem. A* **8**, 388 (2019). https://doi.org/10.1039/c9ta10818a
80. K. Schweinar, O. Kasian, R.L. Nicholls, C.R. Rajamathi, P. Zeller, M. Amati, L. Gregoratti, D. Raabe, M. Greiner, B. Gault, *Microsc. Microanal.* **25**, 306 (2019). https://doi.org/10.1017/S1431927619002265
81. M.K. Miller, K.F. Russell, G.B. Thompson, *Ultramicroscopy* **102**, 287 (2005). https://doi.org/10.1016/j.ultramic.2004.10.011
82. A. BalaKrishnan, N. Blanc, U. Hagemann, P. Gemagami, K. Wonner, K. Tschulik, T. Li, *Angew. Chem. Int. Ed.* **60**(39), 21396 (2021). https://doi.org/10.1002/anie.202106790
83. K. Schweinar, B. Gault, I. Mouton, O. Kasian, *J. Phys. Chem. Lett.* **11**, 5008 (2020). https://doi.org/10.1021/ACS.JPCLETT.0C01258/SUPPL_FILE/JZ0C01258_SI_001.PDF
84. E. Petrishcheva, L. Tiede, K. Schweinar, G. Habler, C. Li, B. Gault, R. Abart, *Phys. Chem. Miner.* **47**, 30 (2020). https://doi.org/10.1007/s00269-020-01097-4
85. B. Gault, M.P. Moody, F. de Geuser, G. Tsafnat, A. La Fontaine, L.T. Stephenson, D. Haley, S.P. Ringer, *J. Appl. Phys.* **105**, 034913 (2009). https://doi.org/10.1063/1.3068197
86. B. Gault, M.P. Moody, J.M. Cairney, S.P. Ringer, *Mater. Today* **15**, 378 (2012). https://doi.org/10.1016/S1369-7021(12)70164-5
87. O. Kasian, S. Geiger, T. Li, J.-P. Grote, K. Schweinar, S. Zhang, C. Scheu, D. Raabe, S. Cherevko, B. Gault, K.J.J. Mayrhofer, *Energy Environ. Sci.* **12**(12), 3548 (2019). https://doi.org/10.1039/c9ee01872g
88. S. Zhang, I. Ahmet, S.-H. Kim, O. Kasian, A.M. Mingers, P. Schnell, M. Kölbach, J. Lim, A. Fischer, K.J.J. Mayrhofer, S. Cherevko, B. Gault, R. Van De Krol, C. Scheu, *ACS Appl. Energy Mater.* **3**, 9523 (2020). https://doi.org/10.1021/acsaem.0c01904
89. A.G. Hufnagel, H. Hajiyani, S. Zhang, T. Li, O. Kasian, B. Gault, B. Breitbach, T. Bein, D. Fattakhova-Rohlfing, C. Scheu, R. Pentcheva, *Adv. Funct. Mater.* **28**(52), 1804472 (2018). https://doi.org/10.1002/adfm.201804472 □

Baptiste Gault is the W2 group leader for atom probe tomography at the Max-Planck-Institut für Eisenforschung, Germany. He received his BS degree from the University of Rouen, France, and completed postdoctoral research in Sydney and Oxford. He is also a part-time professor of atomic-scale characterization in the Department of Materials at Imperial College London, UK. For his pioneering work on atom probe, he received the 2020 Leibniz Prize, the highest scientific distinction in Germany. Gault can be reached by email at b.gault@mpie.de.

Kevin Schweinar is the chief materials scientist at Stat Peel AG. He received his BSc and MSc degrees in applied geosciences from the University of Basel, Switzerland, and RWTH Aachen University, Germany, respectively. He received his PhD degree in materials science from Ruhr-University Bochum, Germany, in 2021. He performed his doctoral research at the Max-Planck-Institut für Eisenforschung GmbH in Düsseldorf, Germany, where he developed and advanced methodological workflows to investigate electrochemically active surfaces by a blend of spectroscopies and microscopies to unveil structure–properties relationships at the atomic level. Schweinar can be reached by email at kevin.schweinar@statpeel.com.

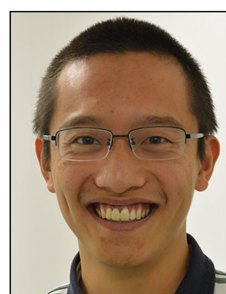

Siyuan Zhang is a project leader at the Max-Planck-Institut für Eisenforschung, Germany, with group activities on microstructural defects and stability of functional materials. He received his BEng degree in materials science and physics from the University of Science and Technology Beijing, China, MSc degree from RWTH Aachen University, Germany, and PhD degree from the University of Cambridge, UK. His research focuses on developing *in operando* and correlative microscopy and spectroscopy techniques to study energy-conversion processes in materials down to atomic resolution. Zhang can be reached by email at siyuan.zhang@mpie.de.

Leopold Lahn is a doctoral candidate at Helmholtz-Zentrum Berlin für Materialien und Energie, Germany, with a focus on structure–function relationships in the oxygen evolution electrocatalysts for long-term stable performance. He studied applied mineralogy and crystallography at the Rheinisch-Westfälische Technische Hochschule Aachen (RWTH Aachen University), Germany. He performed research for his master's thesis on the role of defects in IrRu alloys for energy-conversion applications at the Max-Planck-Institut für Eisenforschung in Düsseldorf. Lahn can be reached by email at leopold.lahn@helmholtz-berlin.de.

Christina Scheu holds a joint position as a professor at the RWTH Aachen University and as an independent research group leader at Max-Planck-Institut für Eisenforschung in Düsseldorf, Germany. From 2008 to 2014, she was a professor at the Ludwig-Maximilian-University, Germany. She received her diploma degree in physics and a PhD degree in materials science. She spent two years as a Minerva Fellow at the Technion—Israel Institute of Technology, Israel. Her expertise is the analysis of functional materials with scanning transmission electron microscopy and electron energy-loss spectroscopy with a focus on interface phenomena and nanostructures. Scheu can be reached by email at scheu@mpie.de.

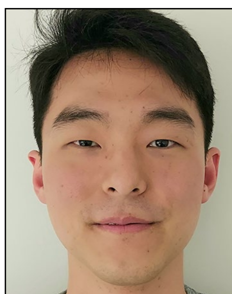

Se-Ho Kim is a postdoctoral researcher at Max-Planck-Institut für Eisenforschung, Germany. He received his bachelor's degree from The University of British Columbia in chemical engineering, his master's degree from the Korea Advanced Institute of Science and Technology, Republic of Korea, and his PhD degree from RWTH Aachen University, Germany, in materials science and engineering. His work has enabled measuring colloidal nanoparticles with atom probe tomography. He now focuses on the design concepts of impurity/dopant engineering for energy materials. Kim can be reached by email at s.kim@mpie.de.

Olga Kasian joined the Friedrich-Alexander-Universität Erlangen-Nürnberg, Germany, as a professor of materials for electrochemical energy conversion. Her current research focuses on the field of electrocatalysis for energy conversion and storage. She received her PhD degree in electrochemistry from the Ukrainian State University of Chemical Technology in 2013. After that, she worked as a postdoctoral researcher at the Brandenburg University of Technology Cottbus-Senftenberg. In 2015, she joined Max-Planck-Institut für Eisenforschung as an Alexander von Humboldt Research Fellow. Since 2019, she has been leading the Helmholtz Young Investigator Group at Helmholtz-Zentrum Berlin focusing on transformations of materials during electrocatalytic reactions. Kasian can be reached by email at olga.kasian@helmholtz-berlin.de.